Biophysical Chemistry 13 (1981) 233–243
North-Holland Publishing Company

LANTHANIDE PROBES IN BIOLOGICAL SYSTEMS: CHARACTERIZATION OF LUMINESCENCE EXCITATION SPECTRA OF TERBIUM COMPLEXES WITH PROTEINS

John DE JERSEY *, Pamela JEFFERS MORLEY and R. Bruce MARTIN
Chemistry Department, University of Virginia, Charlottesville, Virginia 22901, USA

Received 8 December 1980

Upon irradiation in the ultraviolet region aromatic chromophores may transfer energy to a nearby Tb^{3+}, which in turn emits a green phosphorescence. This paper reports the characterization of the ultraviolet excitation spectra of aromatic chromophores capable of transferring energy to Tb^{3+} by monitoring of the green Tb^{3+} emission in the 540–550 nm region. Results are included for complexes containing phenyl, hydroxyphenyl, indole, and catechol chromophores. Characteristic excitation spectra are presented for the aromatic chromophores occurring as side chains in proteins. Though it is preferable to compare entire excitation spectra, the ratio of intensities at 292 to 276 nm, R, is suggested as a useful diagnostic criterion. Numerical R values are indicative of the following aromatic side chains as the energy donor to Tb^{3+}: $R <$ 0.2, unionized tyrosine; R = 0.5 to 1.0, tryptophan; and $R > 1.8$, ionized tyrosine. The phenylalanyl chromophore displays a definitive excitation spectrum at shorter wavelengths. For ovotransferrin R = 0.9 and comparison of the full excitation spectra suggests that it contains comparable contributions from both ionized tyrosine and tryptophan side chains. Some difficulties in obtaining reliable excitation spectra are described. An analysis of inner-filtering of incident light reveals that for an absorbance less than 0.8 the excitation spectrum is broadened and flattened compared to the absorption spectrum. At maximum absorbances greater than 0.8 false maxima may appear to both sides of a real maximum. Two spurious maxima in an excitation spectrum were generated in a Tb^{3+} complex and compared to the correct excitation spectrum of the same complex obtained at lower absorbance.

1. Introduction

Many biological processes involve calcium ions, which commonly exert their effects by binding to proteins. The inapplicability of common spectroscopic techniques to Ca^{2+} has been partly overcome by use of lanthanide ions (Ln^{3+}) as probes. Ca^{2+} resembles Ln^{3+} in size and in preference for oxygen donors in complex formation [1]. Ln^{3+} compete with Ca^{2+} for Ca^{2+} binding sites in many proteins. One of the best spectroscopic Ln^{3+} probes of Ca^{2+} binding sites in proteins is terbium (Tb^{3+}) luminescence.

When excited, Tb^{3+} emits visible light in four spectral bands from 450–650 nm. The most intense of these bands, from 540–550 nm, due to a $^5D_4 \rightarrow {}^7F_5$ transition (phosphorescence), produces a characteristic green emission. The Tb^{3+} emitting $^5D_4$ state may be reached by two methods. Due to the low molar absorptivity of Tb^{3+}, direct excitation requires an intense light source and is relatively insensitive [2]. Potentially more sensitive is indirect or energy transfer excitation in which Tb^{3+} accepts energy by radiationless energy transfer from an efficient energy donor, typically an excited aromatic chromophore. In order for the energy transfer process to be efficient, the energy donor and the Tb^{3+} must be closely spaced. In favorable cases the emission from Tb^{3+} is enhanced by a factor of 10^2–10^6. Enhancement means the ratio of integrated emission intensities due to ligand-bound to free aqueous Tb^{3+}.

Emission resulting from excitation by energy transfer may be usefully considered to occur in four steps, three of which are necessary. 1. A chromophore absorbs radiant energy. 2. The resulting excited state energy is passed rapidly by radiationless energy trans-

* On leave from the Department of Biochemistry, University of Queensland, St. Lucia, Q. 4067, Australia.

0 301–4622/81/0000–0000/S 2.50 © North-Holland Publishing Company

fer to other chromophores. This step is not necessary but occurs readily in proteins and nucleic acids. 3. Energy is transferred, most likely by a dipole–dipole mechanism, from an excited chromophore to a Tb^{3+} 4. Phosphorescence occurs from the Tb^{3+} $^5D_4$ state. By monitoring the intensity of the enhanced green emission band near 545 nm while irradiating the sample, the excitation spectrum so obtained serves to identify the chromophore engaged in energy transfer to Tb^{3+} in step 3 (not necessarily the chromophore that accepted the radiant energy in step 1).

An excitation spectrum characterized by studies on known chromophores serves to identify the chromophore engaged in energy transfer to Tb^{3+} and hence lying close to a Tb^{3+}. Thus there is a potentially powerful tool for identification of aromatic chromophores positioned near Ca^{2+} binding sites in proteins [1,3]. To a first approximation in a solution of sufficiently low absorbance, the excitation spectrum should correspond to the absorption spectrum of the chromophore. In the 240–320 nm region of proteins, four aromatic side chain chromophores could be involved in energy transfer: the phenyl group of phenylalanine (Phe), the indole group of tryptophan (Trp), the phenolic group of tyrosine (Tyr), and the ionized phenolate group of tyrosine (Tyr^-). Since these four chromophores exhibit different absorption spectra in the 240–320 nm region, it should be possible to differentiate among their excitation spectra. Nevertheless, there has been considerable confusion, uncertainty, and incorrect identifications of groups involved in energy transfer to Tb^{3+}.

The principal aim of this research is to characterize the excitation spectra observed in each of the four cases above by studying model complexes and carefully selected Tb^{3+} substituted proteins. With the results of such a characterization, it is possible to identify the aromatic energy donor in Tb^{3+} proteins in which the environment of the metal ion is unknown. The paper also presents a theoretical analysis of the conditions under which spurious maxima appear in excitation spectra. The treatment is supported by observation of spurious maxima in a model complex and in proteins.

2. Materials and methods

$TbCl_3$ was obtained from Alfa-Ventron, mandelic acid from Aldrich Chemical Co., 4,5-dihydroxy-m-benzenedisulfonic acid disodium salt (Tiron) from Eastman Organic Chemicals, and DL-β-phenyllactate, O-methyltyrosine, N-formyltyrosine, o-hydroxyphenylacetic acid, indole-3-lactic acid, *E. coli* alkaline phosphatase (Type III-7; suspension in 2.6 M $(NH_4)_2SO_4$) and α-amylase from *B. subtilis* (Type II A, 4 × crystallized) from the Sigma Chemical Co. The following proteins were gifts: carp muscle parvalbumin from Dr. Donald J. Nelson, Clark University; chicken bone osteocalcin from Dr. Peter Hauschka, Harvard Medical School, bovine brain calmodulin from Dr. Kenneth Seamon, N.I.A.M.D.; and hen ovotransferrin from Dr. Robert Woodworth, University of Vermont. Ethylenedinitrilo-N,N′-bis(2-hydroxyphenyl)-N,N′-diacetate (EHPG) obtained from Pfaltz and Bauer was purified by recrystallization with charcoal treatment. Buffer components were of the best grade obtainable commercially, and pH measurements were made on a Radiometer PHM64 pH meter at 25°. Unless otherwise stated all solutions contained 0.05 M 3-(N-morpholino)propanesulfonate (MOPS) buffer at pH 6.6 made up to 0.10 M ionic strength with KCl.

Concentrations of protein solutions were calculated from their ultraviolet spectra using the following values of $A^{1\%}_{1\,cm}$ and molecular weight: parvalbumin-1.74 at 259 nm, 11,500 [4]; osteocalcin-5.8 at 276 nm, 6,500 [5] calmodulin-2.0 at 280 nm (K. Seamon, personal communication). 16,700 [6]; conalbumin-12 at 280 nm, 76,600 [7]; alkaline phosphatase-7.7 at 280 nm, 89,000 [8]; and α-amylase-25.3 at 280 nm [9], 48,900 [10]. Apo alkaline phosphatase was prepared as described [8]. This treatment conveniently removes Tb^{3+} complexing SO_4^{2-} from the preparation.

Absorption spectra were recorded on a Cary 14 spectrophotometer. Absorbances in figures refer to 1 cm cells. Potentiometric titrations were performed at 25°C using a Radiometer TTT80 titrator, with ABU 80 Autoburette, PHM 64 pH meter and REC 80 Servograph. Fluorimetric experiments were carried out at 25°C on an SLM 8000 spectrofluorimeter combined with an SLM PR-8000 spectrum processing system supplied by SLM Instruments, Urbana, Illinois. The green luminescence of Tb^{3+} was monitored at 544 nm, with excitation in the region of absorbance by the

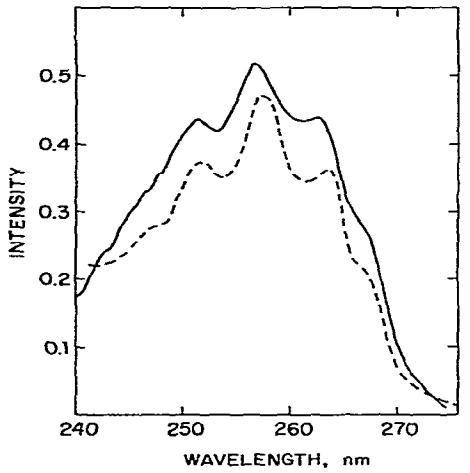

Fig. 1. Absorption (dashed) and Tb^{3+} excitation (solid) spectra of a mixture of mandelic acid (2.3 mM) and Tb^{3+} (0.8 mM) in 0.05 M MOPS buffer, pH 6.60, μ = 0.1; λ_{em} = 544 nm. Ordinate scale refers to absorbance in 1 cm cell.

aromatic chromophore (240 -320 nm). All experiments used the photon counting mode with usual integration times of 20 s. The ratiometric method with rhodamine 6-G in the reference beam was used to correct for variations in lamp intensity with time and wavelength. Semimicro fluorimeter cells (1 ml capacity) were used to decrease effects due to non-productive absorption of the exciting light, giving a path length of 2 mm from the entry point to the center of the cell (from which the emitted light is sampled at right angles to the incident beam). A Corning 3-72 yellow filter was inserted into the emission beam to avoid artifacts caused by second-order scattered light. Titrations of protein solutions with Tb^{3+} were performed by repeated addition of small volumes (5 or 10 μl) of stock aqueous $TbCl_3$ to 1 ml of enzyme in a cell maintained at 25°C in the thermostatted cell holder. When recording excitation spectra, the stability of the samples was routinely checked by measuring intensity at the λ_{max} before and after each run. In no case was an appreciable change observed. Control excitation spectra were run at the same time and under the same conditions omitting either the ligand or the Tb^{3+}. When significant readings were obtained in such control spectra, they were subtracted.

Table 1
Absorption and excitation spectra for Tb^{3+} luminescence [a]

	Absorption	Excitation
Phenylalanine	257.263(0.8) [b]	
Mandelate	256.263(0.8)	257.263(0.8) [b]
β Phenyllactate	257.263(0.8)	259.262(0.8)
Parvalbumin	258.263(0.8)	259.265(0.8)
Tyrosine	275.282(0.83)	
O-Methyltyrosine	273.279(0.85)	274 280(0.83)
N-Formyltyrosine	274.281(0.85)	274.281(0.84)
o-Hydroxyphenylacetate	272.277(0.92)	272.277(0.94)
Calmodulin	276.282(0.84)	276.282(0.86)
Osteocalcin	276.282(0.8)	275.282(0.8)
Tyrosinate (pH 13)	292	
EHPG (pH 9)	292	292
Ovotransferrin (pH 8.5)	280.290(0.7)	282
Tryptophan	278.288(0.83)	278.288(0.8) [c]
Indole-3 lactate	280.288(0.85)	278.288(0.8)
Bacterial α-amylase	280.290(0.7)	275.291(0.6)
Elastase	283.291(0.7)	277.291(0.7)
Porcine trypsin	280.290(0.7)	277.292(0.7)
Chymotrypsin	283.290(0.8)	282.291(0.8)
Tiron : Tb : EDTA (pH 9.8)	271.312(1.3)	315(1.2)

[a] Monitored at 544 nm near pH 6.6 unless otherwise specified.
[b] Number in parentheses is intensity ratio of longer wavelength to shorter wavelength peak listed.
[c] Excitation spectrum without Tb^{3+} with emission monitored at 350 nm.

3. Results

Proteins and model ligands containing aromatic chromophores have been selected to provide examples of the four expected types of excitation spectra of Tb^{3+} protein complexes described in the Introduction. For enhanced Tb^{3+} emission to occur at 544 nm as a result of energy transfer from an aromatic chromophore to Tb^{3+}, there must be some complex formation between the ligand and Tb^{3+}. The choice of ligands was dictated by their relevance and capability of producing at least weak complexes with Tb^{3+} near pH 6.6.

A comparison of the absorption and excitation spectra of a solution containing mandelate (hydroxy-(phenyl)acetate) ions and Tb^{3+} is shown in fig. 1. Potentiometric titration shows that only a small fraction of the mandelate anions is chelated to Tb^{3+} under these conditions, as expected from the low concentrations and weakness of the interaction. The amount of complex is sufficient, however, to produce

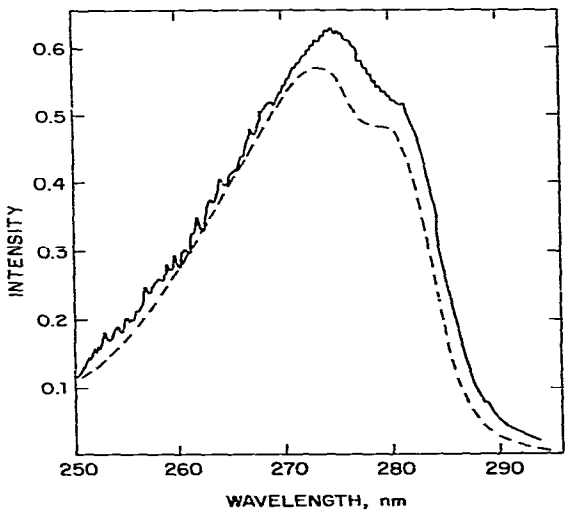

Fig. 2. Absorption spectrum (dashed) and Tb^{3+} excitation spectrum (solid) of a mixture of O-methyltyrosine (0.23 mM) and Tb^{3+} (0.68 mM). Other conditions as in fig. 1.

an informative excitation spectrum which reflects only ligand involved in energy transfer to bound Tb^{3+}. The five peaks and shoulders appearing from 245 to 270 nm in the absorption spectrum also appear at virtually the same wavelengths but with less definition in the excitation spectrum. In both the absorption and excitation spectra the strongest maximum occurs at 257 nm. There are distinct shoulders at 252 and 263 nm. As indicated in table 1 the height of the peak at 263 nm is 0.8 that of the peak at 257 nm. Phenylalanine and β-phenyllactate both yield absorption spectra similar to that of mandelate, and the excitation spectrum of a solution containing β-phenyllactate and Tb^{3+} (3 : 1) is also similar to the excitation spectrum of mandelate (see table 1). Phenylalanine does not form strong enough complexes with Tb^{3+} to give an enhanced Tb^{3+} emission.

Fig. 2 compares the excitation spectrum of a solution of O-methyltyrosine and Tb^{3+} with the absorption spectrum of O-methyltyrosine. Tb^{3+} ions do not produce any significant perturbation of the absorption spectrum. Both the absorption and excitation spectra exhibit a maximum near 274 nm with a shoulder near 280 nm of 0.83 the intensity of the maximum. Results for O-methyltyrosine are summarized in table 1 with those for two other phenol containing ligands, N-formyltyrosine and o-hydroxyphenylacetate. Since the spectra were obtained in a pH 6.6 buffer, in neither of the last two ligands has the phenolic hydrogen undergone deprotonation (confirmed by potentiometric titration). The absorption and excitation spectra for all three ligands are similar and serve to establish characteristics of excitation spectra due to energy transfer from unionized phenolic compounds to Tb^{3+}. Excitation spectra of O-methyltyrosine and N-formyltyrosine were also taken in the absence of Tb^{3+}, with the emission monitored at 305 nm. These excitation spectra are similar to those observed for Tb^{3+} emission at 544 nm upon energy transfer from the same two ligands.

As a representative of the indole side chain of the amino acid tryptophan, a 1 : 3 mixture of 47 μM indole-3-lactate and Tb^{3+} yields some enhancement of Tb^{3+} emission. Absorption and excitation spectra results are recorded in table 1. This excitation spectrum is similar to that of 26 μM L-tryptophan without Tb^{3+} as monitored at 350 nm (table 1). Both excitation and absorption spectra exhibit a characteristic flat maximum from 272–278 nm with a shoulder at 288 nm of 0.8 the intensity of the maximum.

Ionization of the phenolic hydrogen in tyrosine to give the phenolate group is complete by pH 12 [11]. Accompanying the phenolic ionization is a pronounced red shift and intensification of the absorption spectrum with the maximum shifting from 275 to 292 nm (table 1). Due to the strong basicity of the ionized phenolate group, hydroxy complexes of lanthanides occur in aqueous solutions well before phenolate complexation is effective [12]. In other studies requiring complexation of an ionized phenolate, we have employed the hexadentate ligand ethylenedinitrilo-N,N′-bis(2-hydroxyphenyl)-N,N′-diacetate or N,N′-ethylenebis(2-(o-hydroxyphenyl))glycine (EHPG) [7,13]. The neutral ligand contains two carboxylate, two ammonium, and two phenolic groups. The last four groups are titrated from pH 6 to 12 in the free ligand. In the presence of an equimolar amount of Tb^{3+}, the titration is complete by pH 9 and the ligand is hexadentate about Tb^{3+}. In this complex, Tb^{3+} emission at 544 nm is enhanced by a factor of 5 × 10^5 compared with free Tb^{3+} (measured at pH 9.5 with λ_{ex} = 295 nm). This enhancement may be the largest yet observed for a Tb^{3+} complex, and is due in

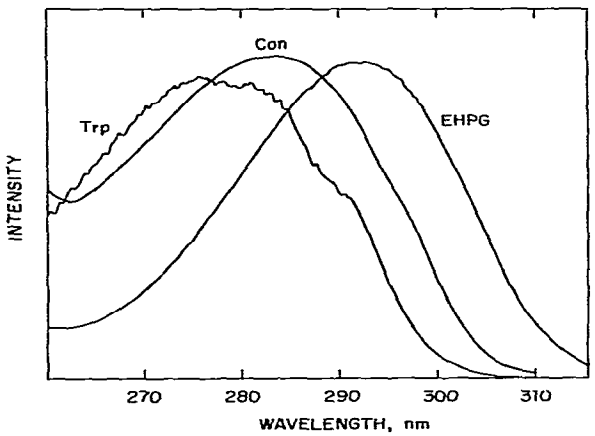

Fig. 3. Excitation spectra monitored at 544 nm for Tb^{3+} complexes of α-amylase (Trp), ovotransferrin (Con) and EHPG. The spectrum of 0.9 μM bacterial α-amylase was obtained at pH 6.6 with 14 equiv Tb^{3+} and that of 4.6 μM ovotransferrin (conalbumin) at pH 8.5 in a tris-HCO_3^- buffer with 0.9 equiv Tb^{3+}. The spectrum of the equimolar EHPG complex was obtained at pH 9.

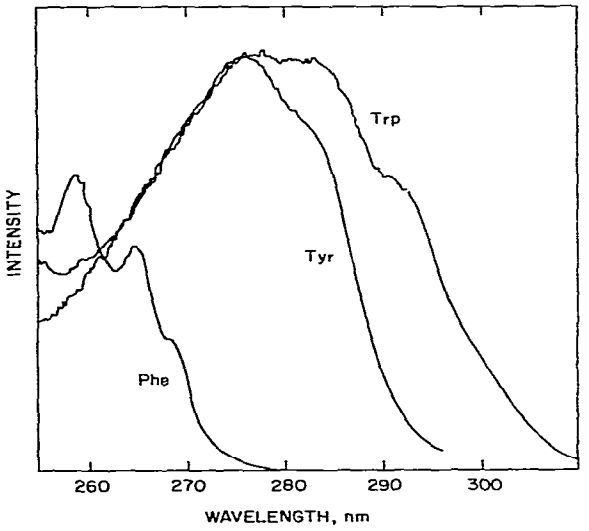

Fig. 4. Excitation spectra of Tb^{3+} proteins with emission monitored at 544 nm: carp parvalbumin (Phe), beef calmodulin (Tyr), and porcine elastase (Trp). All spectra were monitored at pH 6.6 in a MOPS buffer. Other conditions are 69 μM parvalbumin at 1.3 equiv Tb^{3+}, 42 μM calmodulin at 6 equiv Tb^{3+}, and 1.3 μM elastase at 24 equiv Tb^{3+}.

large measure to energy transfer from the two ionized phenolate groups bound to the Tb^{3+}. An excitation spectrum for the equimolar EHPG: Tb^{3+} complex is shown in fig. 3.

The catechol tiron (4,5-dihydroxy-m-benzenedisulfonate) forms a complex with EDTA: Tb^{3+} which potentiometric titration shows to be fully formed by pH 9.8. The hexadentate EDTA holds Tb^{3+} in solution, and on the solvent exposed side of Tb^{3+}, tiron coordinates as a bidentate catecholate. The absorption spectrum exhibits two distinct maxima of similar intensity at 270 nm (ϵ 5700) and 312 (ϵ 7600). In contrast to all other complexes reported in this paper, the excitation spectrum shows a pronounced red shift when compared to the absorption spectrum. In the excitation spectrum the maxima appear at 271 and 315 nm with the longer wavelength peak of substantially greater intensity. Results for this tiron complex appear as the last entry in table 1. It is evident that the excitation spectrum for Tb^{3+} chelated at a catecholate is markedly different from Tb^{3+} complexed at a phenolate (EHPG).

Excitation spectra observed in proteins and considered representative of energy transfer from each of the three aromatic side chains to Tb^{3+} are displayed in fig. 4 and tabulated in table 1. The Ca^{2+} muscle binding protein parvalbumin contains no Tyr or Trp residues and energy transfer to Tb^{3+} in a Ca^{2+} site must be from a Phe residue [14]. The excitation spectrum of parvalbumin closely resembles those for mandelate and β-phenyllactate (table 1).

The excitation spectra for Tb: calmodulin is similar to that of O-methyltyrosine in fig. 2, and represents energy transfer from a tyrosine side chain with an unionized phenolic group. Other examples of energy transfer from tyrosine are osteocalcin [5] (table 1) and troponin-C (TN-C) [15,16]. There is an interesting point of difference between the Tb^{3+} titration curves for TN-C and calmodulin. Most of the enhancement of Tb^{3+} luminescence in TN-C is achieved by addition of the first equivalent of Tb^{3+} [15,16]. In calmodulin, however, the first 2–3 equivalents of Tb^{3+} produced little if any enhancement, and a higher ratio of $[Tb^{3+}]/[protein]$ was required to give significant enhancement. Thus Tb^{3+} luminescence suggests significant differences in calcium binding of the two nearly homologous proteins.

Excitation spectra resulting from energy transfer

from Trp side chains in proteins are typified by the spectra labeled Trp for porcine elastase in fig. 4 and bacterial α-amylase in fig. 3. The excitation spectra for these two proteins, porcine [17], and bovine trypsin, and chymotrypsin are similar and display a broad maximum from 276–282 nm with a shoulder near 292 nm. The results are tabulated near the end of table 1. The utility of Tb^{3+} luminescence as a probe of Ca^{2+} binding to the calcium proteins elastase [18], the trypsins, and chymotrypsin [17] has been described in other papers from this laboratory. Fig. 3 also shows the excitation spectrum for ovotransferrin (conalbumin, Con) upon addition of 0.9 equiv Tb^{3+}.

Luminescence titration of th apoenzyme of *E. coli* alkaline phosphatase with Tb^{3+} ([protein] = 1.64 μM) in 0.01 M Tris-HCl buffer, pH 7.9, gives a curve which corresponds to the binding of one Tb^{3+}/89.000 daltons with an association constant of 6.6×10^6 M^{-1}, similar to that reported by Sherry et al. [8]. A solution in the same buffer 1.5 μM in enzyme and 4.0 μM in Tb^{3+} yields an excitation spectrum with a maximum at 279 nm. The ratio of excitation spectrum intensities at 296 and 279 is 0.53. As indicated in the Discussion section this ratio and the whole excitation spectrum suggests that a tryptophan side chain is the primary group engaged in energy transfer to Tb^{3+}.

4. Inner-filter effects

Inner-filter effects result from absorption of either incident or emitted radiation by the solution. Absorption of emitted light is negligible in this study and is not considered further. Since the intensely absorbing aromatic region of proteins are being excited for energy transfer to Tb^{3+}, absorption of incident radiation necessarily occurs. Only one or a few of many absorbing aromatic side chains are actually involved in energy transfer to Tb^{3+} creating a large background absorption. Without appropriate precautions, inner-filtering of incident radiation may yield spurious peaks in excitation spectra. In the following we demonstrate both theoretically and experimentally how highly absorbing solutions produce spurious peaks in excitation spectra. The analysis begins with a consideration of the effect of inner-filtering of incident radiation on the luminescence spectrum and then considers ramifications for the excitation spectrum. Finally, results of the analysis are used to describe the requirements for obtaining reliable luminescence and excitation spectra.

The treatment that follows assumes that absorption and excitation intensity distributions are closely similar. This assumption appears valid for all systems of this study except possibly the tiron complex. If the assumption does not hold, then the described inner-filter effects will be superimposed on photophysical effects. Portions of the following treatment have been presented [19–21].

In a common experimental set up fluorescence or luminescence is observed at right angles to the path of the incident light. The observation window for emitted light is usually not as wide as the cell containing the solution. We divide the luminescence cell into 3 compartments with two interior planes, labeled 1 and 2, perpendicular to the incident light path that defines the emission window. The boundaries of the solution in the cell are defined by planes 0 and 3 with incident light of intensity I_0 at plane 0 and departing light of intensity I_3 at plane 3. The intensities at the two interior planes 1 and 2 are I_1 and I_2. The luminescence intensity, L, is proportional to the difference in intensities $I_1 - I_2$ and without loss of generality we may write, with K as a proportionality constant

$$L = K(I_1 - I_2)/I_0 = K(10^{-Al_{01}} - 10^{-Al_{02}}). \qquad (1)$$

The second equality in eq. (1) follows from defining A as the absorbance of the solution per cm so that

$$\log(I_i/I_0) = -Al_{0i} = -\epsilon c l_{0i}.$$

where l_{0i} is the path length between planes 0 and i in cm, ϵ the molar absorptivity, and c the molar concentration. The absorbance per cm measured in an absorption spectrophotometer spans the entire width of solution in the cell, l_{03}, and is given by $\log(I_0/I_3) = Al_{03}$.

The distances that appear in eq. (1), l_{01} and l_{02}, are those from the incident plane 0 to the planes defining the limits of the emission window for emitted light. The positions of planes 1 and 2 are not often known with precision. Therefore, we express these distances in terms of the accurately known distance l_{03}. To do so we define the ratio

$$f = l_{12}/l_{03} = l_{12}/b,$$

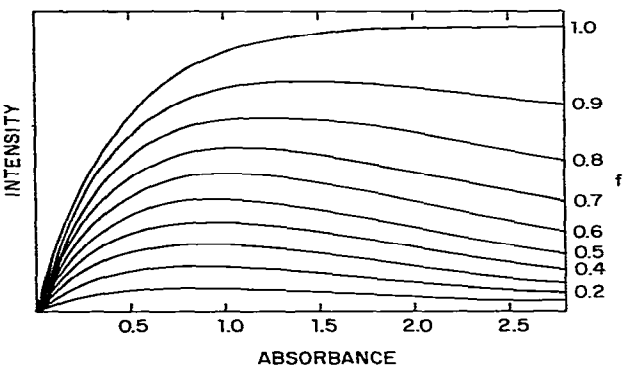

Fig. 5. Luminescence intensity, L, versus absorbance through the cell, Ab, for designated fractions f on the right. The fraction f is the ratio of the width of the cell-centered emission window to the width of the solution in the luminescence cell.

which describes the fraction of the entire solution width in the cell $l_{03} \equiv b$, taken up by the emission window, l_{12}. Values of f vary from 0 for no emission window to 1 for a window that spans the entire width of solution in the cell. In many fluorescence spectrometers, including ours, the emission window is centered in the cell so that lengths $l_{01} = l_{23}$. Though the treatment that follows depends quantitatively on the assumption of a cell-centered emission window, it would require little modification to apply to situations where the emission window is not cell-centered, and the conclusions are qualitatively similar to those derived from other geometries. For cell-centered emission windows and the above definitions we obtain $l_{01} = l_{03}\,(1-f)/2$ and $l_{02} = l_{03}\,(1+f)/2$. Relabeling the entire width of solution in the cell, $l_{03} = b$, and substituting into eq. (1) we obtain

$$L = K(10^{-Ab(1-f)/2} - 10^{-Ab(1+f)/2}), \qquad (2)$$

In the limit of a vanishingly narrow emission window, $f \to 0$ and $L \to 0$. When the emission window becomes as wide as the solution in the cell, $f = 1$, and $L = K(1 - 10^{-Ab})$. The term in parentheses may be expanded in the series $Ab \ln 10 - (Ab \ln 10)^2/2! + \ldots$. It is on the basis of the first term in this expression that luminescence intensity, L, is often assumed to be proportional to the absorbance of a solution, Ab. This proportionality of $L \sim Ab$ is valid, however, only in the limit of low absorbances, $Ab < 0.1$. The limiting slope of $1 - 10^{-x}$ versus x as $x \to 0$ is $\ln 10 = 2.30$. At $x = 0.1$ this slope is already reduced to 2.06 and at $x = 0.2$ it is 1.85. At higher values of $Ab > 0.2$ the slope continues to decrease and greater extents of "inner-filtering" occur as the luminescence intensity, L, is no longer proportional to absorbance, Ab.

The dependence of luminescence intensity, L, as a function of cell absorbance through the cell, Ab, according to eq. (2) is shown in fig. 5. Each curve corresponds, in intervals of 0.1, to a fraction f from 0.1 to 1.0 of the entire solution width in the cell taken up by the cell-centered emission window. The curve for $f = 0$ is coincident with the abscissa. Fig. 5 shows graphically that only at low absorbances, $Ab < 0.2$ and high emission window fractions, $f > 0.7$ is the luminescence intensity even approximately proportional to absorbance. A maximum appears in all curves of fig. 5, except that for $f = 1.0$. Differentiation of eq. (2) indicates that the maximum appears at $(Ab)_{max} = (1/f) \log((1+f)/(1-f))$. In the limit of $f \to 0$ the limit of $(Ab)_{max} = 2/\ln 10 = 0.8686$. With increasing f the maxima move only slowly to higher Ab values, at $f = 0.5$, $(Ab)_{max} = 0.95$; at $f = 0.6$, $(Ab)_{max} = 1.00$, at $f = 0.8$, $(Ab)_{max} = 1.19$, and even at $f = 0.9$, $(Ab)_{max} = 1.42$. The presence of the maxima in the curves of fig. 5 means that solutions with absorbances greater than the maximum absorbance for a given f value will display weaker luminescence than solutions with absorbances nearer the maximum value, which is $(Ab) \sim 0.9$ for $f = 0.0$ to 0.5.

Ramifications of the features of fig. 5 have important applications for the procurement of reliable excitation spectra. An excitation spectrum reflects the response in emitted light intensity as the exciting wavelength is scanned through an absorption band. Theoretical curves of excitation spectra versus frequency appear in fig. 6. The curves were constructed by assuming an absorption spectrum gaussian in frequency and applying eq. (2) across the absorption band. Solutions for 6 different maximum absorbance values are denoted on the curves in fig. 6. All the curves drawn are for an emission window to whole solution width $f = 0.5$. Similar curves are obtained at other f values except for those at $f = 1.0$ where no maxima but only flattening appears, becoming pronounced at $Ab > 0.4$. For $f = 0.5$ the maximum in fig. 5 occurs at $Ab = 0.95$. As a consequence in fig. 6 only the two curves with a maximum Ab of 0.1 and 0.6 appear normal. Actually

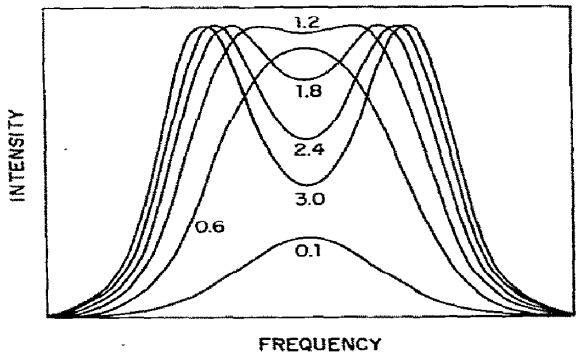

Fig. 6. Excitation spectra intensity versus frequency for $f = 0.5$ at indicated values of the maximum absorbance in an absorption band.

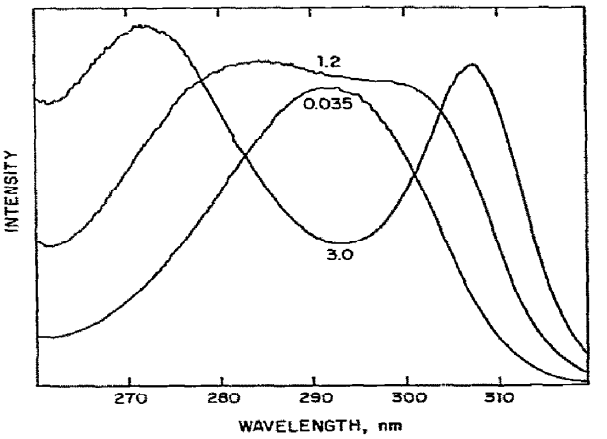

Fig. 7. Excitation spectra of equimolar complex of EHPG and Tb^{3+} at pH 9. The intensity scale is arbitrary. Numbers and curves refer to absorbances, Ab, of the solutions: 0.035 0.011 mM complex in 4 mm cell; 1.2, 0.38 mM complex in 4 mm cell; and 3.0. 0.38 mM complex in 10 mm cell. At pH 9 the absorption spectrum resembles the curve labeled 0.035 in shape and shows a maximum at 292 nm with $\epsilon = 7800$. The excitation spectrum of the curve labeled 0.035 also appears in fig. 3.

the 0.6 curve is notably topped and hence flattened. The maximum in the $Ab = 0.6$ curve occurs at only 3.4 instead of 6.0 times the intensity of the $Ab = 0.1$ curve. For the four curves of highest Ab in fig. 6, a depression appears in the excitation spectra at all values where $Ab > 0.95$. Such pronounced inner-filtering of the absorbed radiation gives rise to excitation spectra with two spurious peaks, one to each side of the position of the absorption maximum. Such spurious peaks will occur when the maximum absorbance exceeds 1.0 for $f \leqslant 0.6$, 1.2 for $f = 0.8$, and 1.4 for $f = 0.9$. To avoid the appearance of spurious maxima, excitation spectra should never be taken in solutions with maximum absorbances greater than 0.8.

Experimental excitation spectra similar to the double peaked theoretical curves in fig. 6 are easily realizable, and inadvertent examples appear in the literature. The theoretical curve with $Ab = 3.0$ in fig. 6 is plotted because the maximum absorbance corresponds to that of the solution of the Tb^{3+} complex of EHPG, the excitation spectrum of which is the pronounced double peaked curve, also labeled 3.0, in fig. 7. Numbers on curves in fig. 7 represent absorbances of the solutions. The similarities between the theoretical and experimental curves are evident: the spurious maximum at 307.5 nm in fig. 7 has the characteristics anticipated from the $Ab = 3.0$ curve in fig. 6. The shorter wavelength region of the double peaked curve in fig. 7 is distorted by an additional absorption band at still shorter wavelengths. The flattest excitation spectrum in fig. 7 corresponds closely to the theoretical curve for 1.2 absorbance in fig. 6. The remaining simple curve in fig. 7 is the excitation spectrum for a solution with absorbance of only 0.035 and offers the most reliable excitation spectrum for Tb^{3+} and EHPG. (It is this last curve that is shown for EHPG in fig. 3.) It corresponds in shape to the theoretical curve for 0.1 absorbance in fig. 6. Thus each of the experimental curves in fig. 7 finds its close theoretical counterpart in fig. 6.

Two excitation spectra maxima for Tb^{3+} luminescence have been reported at 295 and near 260 nm for a solution containing 0.1 mM porcine trypsin [22]. The maximum absorbance for this solution is estimated to be 3.5. At this high absorbance we predict a pair of spurious maxima at all f values <0.9994. The excitation spectrum for Tb^{3+} luminescence from porcine trypsin obtained in this research appears in ref. [17] and is similar to those labeled Trp for α-amylase in fig. 3 and elastase in fig. 4. As indicated in table 1, the excitation spectrum of porcine trypsin shows a maximum at 277 nm with a tryptophan shoulder at 292 nm. As anticipated from fig. 6, the true excitation spectrum maximum at 277 nm is nearly midway between the pair of reported spurious maxima at 260 and 295 nm.

The preceding discussion with the results of figs. 5 and 6 suggests the requirements and desirable conditions for obtaining reliable luminescence and excitation spectra. Spurious peaks will be avoided in an apparatus with a cell-centered emission window if the maximum absorbance in the excitation region is less than 0.8. Even so, luminescence and excitation spectra taken at high absorbances will not be proportional to those obtained at lower absorbances. This conclusion is demonstrated by the lack of proportionality by almost a factor of 2 between the two curves at 0.1 and 0.6 absorbance in fig. 6. In a luminescence experiment the absorbance should be as low as practical. A helpful way to reduce inner-filter effects due to incident radiation is to minimize the distance l_{01} between the front face of the cell and the first plane of the emission window. This reduction may be done in two ways. Narrow width cells may be used. In all research in this study (except the deliberate exception in fig. 7) cells only 0.4 cm wide were employed. This technique increases f in a cell-centered emission window. Alternatively, in an apparatus that permits it, the emission window may be moved closer to the front surface of the cell where the irradiating light is incident.

5. Discussion

This research successfully delineates diagnostic criteria for characterization of protein chromophores engaged in energy transfer to Tb^{3+} leading to its emission in the visible spectrum. Fig. 4 displays excitation spectra observed in proteins which may be taken as prototypes for energy transfer from each of the three aromatic side chains. Energy transfer from Phe is demonstrated in parvalbumin, from Tyr (nonionized) in calmodulin, and from Trp in elastase. The expected excitation spectrum due to energy transfer from an ionized phenolate side chain in Tyr is indicated by the spectrum of EHPG : Tb^{3+} in fig. 3. The side chain chromophore engaged in energy transfer to Tb^{3+} in an unknown protein may be deduced by comparison of its excitation spectrum with the prototype spectra of figs. 3 and 4. Though the imidazole side chain of histidine is also aromatic, it is unlikely that it will contribute to Tb^{3+} excitation spectra in the 250–310 nm region.

Absorption spectra for proteins are composites over all aromatic side chains present. The absorption bands are usually shifted to the red compared to bands of the constituent amino acids in aqueous solutions. Excitation spectra reflect only the one or two side chains engaged in significant energy transfer to Tb^{3+}. This excitation spectra in proteins should not be compared with absorption spectra of individual amino acids or of the whole protein but rather to representative excitation spectra in figs. 3 and 4 due to energy transfer to Tb^{3+} from specified aromatic side chains in proteins.

Comparison of the complete excitation spectrum of an unknown Tb^{3+} protein with the four prototype spectra in figs. 3 and 4 provides the best way to indicate the aromatic side chain engaged in energy transfer to Tb^{3+}. The distinction between Tyr and Trp depends upon appreciable intensity or even a shoulder with Trp at about 292 nm, where there is little intensity with Tyr. For all the small ligands and proteins we have investigated, the ratio, R, of excitation spectra intensities at 292 to 276 nm is <0.2 for Tyr and from 0.5 to 0.8 for Trp. Phe displays no appreciable excitation spectrum at either wavelength, and fig. 4 shows that its excitation spectrum is unique and easily recognized. For the ionized phenolate side chain of EHPG, $R = 2.0$. We suggest the simple diagnostic guideline that for the ratio, R, of excitation spectrum intensities at 292 to 276 nm the side chain engaged in energy transfer to Tb^{3+} is indicated as follows: $R <$ 0.2, nonionized Tyr; $0.5 < R < 1.0$, Trp; and $R > 1.8$, ionized Tyr $^-$.

Because of the possibility of hydroxo complex formation, it is desirable to perform experiments with Tb^{3+} at $pH < 7$ [12]. At $pH < 7$ there will be few instances in which tyrosyl side chains have undergone deprotonation even in the presence of metal ions. If it is necessary to have $pH > 7$, excess aqueous Tb^{3+} should be avoided.

There is strong evidence of several kinds that in transferrin and ovotransferrin (conalbumin) two metal ions, such as Fe^{3+}, Cu^{2+}, and Tb^{3+}, are bound per 76,600 Dalton unit via ionized phenolate groups of tyrosyl side chains [7,23–25]. As shown in fig. 3, the excitation spectrum of Tb^{3+}-substituted ovotransferrin at pH 8.5 is an imperfect match to that of EHPG : Tb^{3+}, where two phenolate oxygens coordinate to Tb^{3+}. The ratio of Tb^{3+} to ovotransferrin in the experiment of fig. 3 was only 0.9, so that there

should not be a contribution from Tb^{3+} bound at other sites. With both $R = 0.9$ and an excitation spectrum in fig. 3 intermediate between the Trp and Tyr^- cases, ovotransferrin appears to represent an interesting special case. There are at least three explanations that might account for the intermediate ovotransferrin excitation spectrum. For some reason the protein environment results in a blue shift of the excitation spectrum. Second, the ortho hydroxy groups in EHPG may be a poor model for para hydroxy groups in tyrosyl side chains. Finally, comparison of the three excitation spectra in fig. 3 suggests that the one for ovotransferrin contains comparable contributions from both Tyr^- and Trp side chains. According to this experiment, there is at least one Trp chain near enough to at least one of the two strong metal ion sites of ovotransferrin to be engaged in efficient energy transfer to Tb^{3+}. This proposal receives some support from the quenching by Tb^{3+} of some transferrin fluorescence, which is due to tryptophan [24], and to a metal ion induced difference spectrum perturbation assigned to Trp [26].

The realized enhancement of Tb^{3+} emission in the 540–550 nm region may be less from a bound ionized phenolate than from an unbound tryptophan side chain. It is interesting to compare the high enhancement of 5×10^5 (λ_{ex} = 295 nm) found for the EHPG : Tb^{3+} complex with that of 2×10^4 (λ_{ex} = 283 nm) for elastase [17]. When allowance is made for two bound ionized phenolate rings in the EHPG complex and the approximately 6 times stronger intensity in the excitation spectrum of aqueous Tb^{3+} at 283 nm compared to 295 nm, the enhancement considered to occur from a single Trp in elastase is about half that assigned to a single phenolate ring of EHPG. The number of Tb^{3+} bound water molecules may be different in the two cases and provide differing probabilities for radiationless deactivation. Nevertheless, it appears that energy transfer to Tb^{3+} from an unbound Trp side chain may be comparable in efficiency to that of a bound ionized phenolate.

Excited state energy in a protein flows from Phe → Tyr → Trp [27]. Thus even if a Phe ring is involved in the absorption process of step 1 (see Introduction), the excitation energy is rapidly passed among other Phe rings [28] and transmitted to Tyr and Trp side chains. The excitation spectrum only identifies the side chain involved in energy transfer to Tb^{3+}. Since it absorbs relatively weakly, energy transfer from Phe would normally not be evident in the presence of even modest transfer from Tyr and Trp. Because of greater overlaps between Tb^{3+} absorption and luminesence from Trp than from Phe or Tyr in the 330–400 nm region, energy transfer from Trp will be much more efficient than from Phe or Tyr (nonionized). This conclusion is supported by the predominance of energy transfer from Trp in more than 20 proteins [3] even though it is rarely the most prevalent aromatic side chain in a protein.

Characterization of the Tb^{3+} emission spectra that occurs upon excitation of aromatic residues in proteins provides a baseline for further studies in more complex systems. It remains to be shown whether binding of nucleic bases and other aromatic chromophores to proteins will be near enough to Tb^{3+} binding sites to alter enhancements and impose new imprints on excitation spectra.

Acknowledgement

We thank Drs. Donald J. Nelson, Peter Hauschka, Kenneth Seamon, and Robert Woodworth for protein samples. This research was supported by grants from the National Institute of General Medical Sciences (GM24875) and the National Science Foundation.

References

[1] R.B. Martin and F.S. Richardson, Quart. Rev. Biophysics 12 (1979) 181.
[2] W.D. Horrocks, Jr., G.F. Schmidt, D.R. Sudnick, C. Kittrell and R.A. Bernheim, J. Am. Chem. Soc. 99 (1977) 2378.
[3] H.G. Brittain, F.S. Richardson and R.B. Martin, J. Am. Chem. Soc. 98 (1976) 8255.
[4] D.J. Nelson, T.L. Miller and R.B. Martin, Bioinorg. Chem. 7 (1977) 325.
[5] P.V. Hauschka and P.M. Gallop, in: Calcium-binding proteins and calcium function, ed. R.H. Wasserman (North-Holland, N.Y. 1977) p. 338.
[6] D.J. Wolff and C.O. Brostrom, Adv. Cyc. Nucl. Res. 11 (1979) 27.
[7] R. Prados, R.K. Boggess, R.B. Martin and R.C. Woodworth, Bioinorg. Chem. 4 (1975) 135.
[8] A.D. Sherry, S. Au-Young, and G.L. Cottam, Arch. Biochem. Biophys. 189 (1978) 277.

[9] J. Hsui, E.H. Fischer and E.A. Stein, Biochemistry 3 (1964) 61.
[10] T. Takagi, H. Toda and T. Isemura, Enzymes 3rd Ed. 5 (1971) 235.
[11] R.B. Martin, J.T. Edsall, D.B. Wetlaufer and B.R. Hollingworth, J. Biol. Chem. 233 (1958) 1429.
[12] R. Prados, L.G. Stadtherr, H. Donato, Jr., and R.B. Martin, J. Inorg. Nucl. Chem. 36 (1974) 689.
[13] R.K. Boggess and R.B. Martin, J. Am. Chem. Soc. 97 (1975) 3076.
[14] H. Donato, Jr. and R.B. Martin, Biochemistry 13 (1974) 4575.
[15] T.L. Miller, D.J. Nelson, H.G. Brittain, F.S. Richardson, R.B. Martin and C.M. Kay, FEBS Lett. 58 (1975) 262.
[16] H.G. Brittain, F.S. Richardson, R.B. Martin, L.D. Burtnick and C.M. Kay, Biochem. Biophys. Res. Commun. 68 (1976) 1013.
[17] J. de Jersey, R. Lahue and R.B. Martin, Arch. Biochem. Biophys. 205 (1980) 536.
[18] J. de Jersey and R.B. Martin, Biochemistry 19 (1980) 1127.
[19] W.E. Ohnesorge, Analyt. Chim. Acta 31 (1964) 484.
[20] C.A. Parker and W.J. Barnes, Analyst 82 (1957) 606.
[21] J.F. Holland, R.E. Teets, P.M. Kelly and A. Timnick, Anal. Chem. 49 (1977) 706.
[22] M. Epstein, J. Reuben and A. Levitzki, Biochemistry 16 (1977) 2449.
[23] R.C. Warner and I. Weber, J. Am. Chem. Soc. 75 (1953) 5094.
[24] C.K. Luk, Biochemistry 10 (1971) 2838.
[25] A. Gafni and I.Z. Steinberg, Biochemistry 13 (1974) 800.
[26] A.T. Tan and R.C. Woodworth, Fed. Proc. 27 (1968) 780.
[27] J.W. Longworth, in: Excited states of proteins and nucleic acids, eds. R.F. Steiner and I. Weinryb (Plenum Press, New York, 1971).
[28] E.A. Burstein, E.A. Permyakov, V.I. Emelyanenko, T.L. Bushueva and J.F. Pechere, Biochem. Biophys. Acta 400 (1975) 1.